

Hall conductance of two-band systems in a quantized field

Z. C. Shi^{1,2}, H. Z. Shen^{1,2}, and X. X. Yi¹ *

¹Center for Quantum Sciences and School of Physics, Northeast Normal University, Changchun 130024, China

²School of Physics and Optoelectronic Technology, Dalian University of Technology, Dalian 116024, China

Kubo formula gives a linear response of a quantum system to external fields, which are classical and weak with respect to the energy of the system. In this work, we take the quantum nature of the external field into account, and define a Hall conductance to characterize the linear response of a two-band system to the quantized field. The theory is then applied to topological insulators. Comparisons with the traditional Hall conductance are presented and discussed.

PACS numbers: 03.65.Yz, 05.30.Rt, 03.67.Pp

I. INTRODUCTION

The integer quantum Hall effect (IQHE) is manifested by a remarkably precise quantization of the transverse conductance in two-dimensional electron systems in presence of a strong perpendicular magnetic field. Its discovery [1, 2] has had profound implications for the understanding of matter, and it may find potential applications in quantum information processing [3]. The integer quantum Hall effects can be understood in the single particle framework [4, 5]: Charged particles in a magnetic field form Landau levels with energy splitting that is proportional to the strength of the magnetic field, and when an integer number of Landau levels are filled, the Hall conductance is quantized and characterized by the TKNN number [6] that is now treated as a topological invariant called Chern number. This topological understanding of the IQHE is a remarkable step of progress, opening up the field of topological electronic states in condensed matter physics. Later, Haldane [7] found that a periodic 2D honeycomb lattice without net magnetic flux can in principle support a similar integer quantum Hall effect. This result suggested that certain materials, other than the 2D electron gas under magnetic field, can have topologically non-trivial electronic band structures, which can be characterized by a non-zero Chern number. Such materials are called topological insulators now.

In contrast to ordinary band insulators, topological insulator [9–11] comes with gapless chiral edge states that each carries a quantum of conductance, $\frac{e^2}{h}$. The number of edge states is mathematically given by the value of the topological invariant, namely the Chern number, that can only assume integer values similar to winding numbers. The integer nature of the Chern number is what makes the edge states, and hence the quantization of the conductivity.

Physically, the quantized conductance can be derived by linear response theory. In the context of quantum statistics, the exposition of the linear response theory can be found in the paper by Ryogo Kubo [12], which defines particularly the Kubo formula. This formula gives a linear response of quantum systems to external classical fields. Particularly, it considers the response to a classically electric field of an other-

wise stationary observable, say current. The goal for us in this work is to answer the following question: When the field is quantized, how a quantum system responds to that field?

The answer to this question is not trivial. Firstly, this answer conceptually contributes to the broader question of how quantum systems respond to a quantized driving. A simple setting is provided by a two-band model (that can describe TIs) driven by a single mode electromagnetic field with frequency ω , with the Hall current denoting the response to the driving. Secondly, the answer extends the theory of adiabatic response of quantum systems undergoing unitary evolution [13, 14] to bipartite quantum systems consisting of a quantum system and a quantum driving field [15–18]. As a result, the presented formalism opens a remarkable new area for response theory, where condensed matter physics and quantum optics meet.

II. FORMALISM

As a starting point, let us consider a generic two-band Hamiltonian,

$$H_0(\vec{k}) = \vec{d}(\vec{k}) \cdot \vec{\sigma} + \epsilon(\vec{k}) \cdot \mathbf{I}, \quad (1)$$

where \mathbf{I} is the 2×2 identity matrix, $\vec{\sigma} = (\sigma_x, \sigma_y, \sigma_z)$ are Pauli matrices, $\epsilon(\vec{k})$ and $\vec{d}(\vec{k})$ depend on the materials under study and determine its band structure. The two bands may describe different physical degrees of freedom. If they are the components of a spin-1/2 electron, $\vec{d}(\vec{k})$ stands for the spin-orbit coupling. If they denote the orbital degrees of freedom, then $\vec{d}(\vec{k})$ represents the hybridization between bands. The discussion below is completely independent of the physical interpretation of the Hamiltonian Eq. (1), and leads to a general formalism regarding the two-band system.

In the next section, we will specify $\epsilon(\vec{k})$ and $\vec{d}(\vec{k})$ to examine the response of a concrete quantum system to a quantum driving field. In the presence of an electromagnetic field represented by vector potential \vec{A} of frequency ω , by changing the crystal momentum, $\vec{k} \rightarrow (\vec{k} - \frac{e}{\hbar} \vec{A})$, we can still use the two-band model to describe the system in the field. In the weak field limit, we may expand the Hamiltonian up to the first or-

*Corresponding address: yixx@nenu.edu.cn

der in \vec{A} ,

$$H = H_0(\vec{k} - \frac{e}{\hbar}\vec{A}) \simeq H_0(\vec{k}) - \frac{e}{\hbar} \sum_{j=x,y,z} (\nabla d_j \cdot \vec{A}) \cdot \sigma_j. \quad (2)$$

In the Hilbert space spanned by the eigenstates of σ_z , satisfying $\sigma_z|\uparrow\rangle = +|\uparrow\rangle$, $\sigma_z|\downarrow\rangle = -|\downarrow\rangle$, the eigenvalues and the corresponding eigenstates of $H_0(\vec{k})$ take, $\varepsilon_{\pm} = \epsilon(\vec{k}) \pm |\vec{d}|$ and $|\varepsilon_+\rangle = \cos\frac{\theta}{2}e^{-i\phi}|\uparrow\rangle + \sin\frac{\theta}{2}|\downarrow\rangle$, $|\varepsilon_-\rangle = \sin\frac{\theta}{2}e^{-i\phi}|\uparrow\rangle - \cos\frac{\theta}{2}|\downarrow\rangle$. Here, $|\vec{d}| = \sqrt{d_x^2 + d_y^2 + d_z^2}$, $\cos\theta = \frac{d_z}{|\vec{d}|}$, and $\tan\phi = \frac{d_y}{d_x}$.

Taking the field to be in the x -direction, $\vec{A} = (A_x, 0, 0)$, and decomposing the field in a mean amplitude \bar{E} and a quantum part, $\delta_E(a^\dagger + a)$, i.e.,

$$A_x = E_x t = \bar{E}t + \delta_E(a^\dagger + a)t, \quad (3)$$

we write the Hamiltonian as,

$$H = |\vec{d}|\tau_z + (g_c|\varepsilon_+\rangle\langle\varepsilon_-|e^{i\omega t} + h.c.) + [g_q|\varepsilon_+\rangle\langle\varepsilon_-|(a^\dagger e^{-i\omega t} + a e^{i\omega t}) + h.c.]. \quad (4)$$

Here $g_c \equiv ie\bar{E}\langle\varepsilon_+|\frac{\partial\varepsilon_-}{\partial k_x}\rangle$, $g_q \equiv ie\delta_E\langle\varepsilon_+|\frac{\partial\varepsilon_-}{\partial k_x}\rangle$. $\tau_+ \equiv |\varepsilon_+\rangle\langle\varepsilon_-|$, $\tau_- \equiv \tau_+^\dagger$, and $\tau_z \equiv |\varepsilon_+\rangle\langle\varepsilon_+| - |\varepsilon_-\rangle\langle\varepsilon_-|$. \bar{E} and δ_E are real, a^\dagger and a stands for the creation and annihilation operator of the quantum part of the field.

In terms of eigenstates of H_c defined by $H_c \equiv |\vec{d}|\tau_z + (g_c|\varepsilon_+\rangle\langle\varepsilon_-|e^{i\omega t} + h.c.)$, the Hamiltonian can be rewritten as,

$$H = \sum_{j=+,-} E_j^c |E_j^c\rangle\langle E_j^c| + \hbar\omega a^\dagger a + \eta(a^\dagger + a)|E_+^c\rangle\langle E_-^c| + h.c.. \quad (5)$$

Here, $\eta = -g_q \cos^2\frac{\alpha_c}{2}e^{-i\beta_c} + g_q^* \sin^2\frac{\alpha_c}{2}e^{i\beta_c}$, $E_{\pm}^c = \pm\sqrt{(|\vec{d}| - \frac{\hbar\omega}{2})^2 + |g_c|^2}$, $|E_+^c\rangle = \cos\frac{\alpha_c}{2}e^{i\beta_c}|\varepsilon_+\rangle + \sin\frac{\alpha_c}{2}|\varepsilon_-\rangle$, and $|E_-^c\rangle = \sin\frac{\alpha_c}{2}e^{i\beta_c}|\varepsilon_+\rangle - \cos\frac{\alpha_c}{2}|\varepsilon_-\rangle$. $\cos\alpha_c = \frac{2|\vec{d}| - \hbar\omega}{\sqrt{(2|\vec{d}| - \hbar\omega)^2 + 4|g_c|^2}}$, $\tan\beta_c = \Im(g_c)/\Re(g_c)$ with $\Im(\dots)$ and $\Re(\dots)$ denoting the imaginary and real part of (...), respectively.

Under the rotating-wave approximation(RWA), the eigenstate and the corresponding eigenvalues take,

$$|E_{\pm}^q\rangle_n = \cos\frac{\alpha_q^\pm}{2}e^{i\beta_q}|E_+^c\rangle \otimes |n\rangle + \sin\frac{\alpha_q^\pm}{2}|E_-^c\rangle \otimes |n+1\rangle, \quad (6)$$

where $\cos\alpha_q^+ = \frac{\Delta}{\sqrt{\Delta^2 + 4|\eta|^2(n+1)}}$, $\alpha_q^- = \alpha_q^+ - \pi$, $\tan\beta_q = \frac{\Im(\eta)}{\Re(\eta)}$, and $\Delta = 2E_+^c - \hbar\omega$. $|n\rangle$ denotes a Fock state of the field. The results beyond the RWA will be given in Appendix. Using the relation $v_y = \frac{1}{\hbar}\frac{\partial H(\vec{k})}{\partial k_y}$, we easily find $v_y = \frac{\hbar k_y}{m^*} + \sum_{j=x,y,z} \frac{\partial d_j}{\hbar\partial k_y} \cdot \sigma_j$. Then the y -component of the average velocity in state $|E_-^q\rangle$ is given by,

$$\begin{aligned} \bar{v}_y &= {}_n\langle E_-^q | v_y | E_-^q \rangle_n \\ &= \sin^2\frac{\alpha_q^-}{2} \langle E_+^c | v_y | E_+^c \rangle + \cos^2\frac{\alpha_q^-}{2} \langle E_-^c | v_y | E_-^c \rangle \\ &= -\cos\alpha_q^- \Re(\sin\alpha_c e^{-i\beta_c} \langle \varepsilon_+ | v_y | \varepsilon_- \rangle). \end{aligned} \quad (7)$$

Consider the system under an external electric field $E_x \neq 0$ without magnetic field. The dc current density $j(\bar{E}, \delta_E, n) = j_y(\bar{E}, \delta_E, n)$ can be then obtained from the equation given above by,

$$j_y(\bar{E}, \delta_E, n) = -e \int \frac{dk_x dk_y}{(2\pi)^2} \bar{v}_y \Big|_{\omega \rightarrow 0}. \quad (8)$$

For the quantum part of the field, a linear response of the system to the photon number in the field is then defined by,

$$\sigma_n = \frac{\partial j(\bar{E}, \delta_E, n)}{\partial n} \Big|_{n \rightarrow 0}. \quad (9)$$

After some straightforward algebra, and expanding σ_n up to the first order in \bar{E} , we have

$$\sigma_n = \frac{e^2 \bar{E}}{\hbar} \int \frac{idk_x dk_y}{(2\pi)^2} \frac{\partial \cos\alpha_q^-}{\partial n} \Big|_{n=0} \left[\left\langle \frac{\partial \varepsilon_-}{\partial k_x} \middle| \frac{\partial \varepsilon_-}{\partial k_y} \right\rangle - \left\langle \frac{\partial \varepsilon_-}{\partial k_y} \middle| \frac{\partial \varepsilon_-}{\partial k_x} \right\rangle \right]. \quad (10)$$

Noticing that the Berry curvature of the lower bare band $|\varepsilon_-\rangle$ is defined by $\Omega_{xy}^-(\vec{k}) = i \left[\left\langle \frac{\partial \varepsilon_-}{\partial k_x} \middle| \frac{\partial \varepsilon_-}{\partial k_y} \right\rangle - \left\langle \frac{\partial \varepsilon_-}{\partial k_y} \middle| \frac{\partial \varepsilon_-}{\partial k_x} \right\rangle \right]$, we find that σ_n is simply the BZ integral of the Berry curvature weighted by the factor $\frac{\partial \cos\alpha_q^-}{\partial n} \Big|_{n=0}$. Discussions on Eq. (10) are in order.

Consider a limit of $\Delta \gg 4|\eta|^2(n+1)$, $\cos\alpha_q^- \sim \frac{2|\eta|^2(n+1)}{\Delta^2} - 1$, then $\sigma_n \simeq \frac{e^2 \bar{E}}{\hbar} \frac{2|\eta|^2}{\Delta^2} C_n$. Here, we assume $\frac{2|\eta|^2}{\Delta^2}$ independent of \vec{k} , and C_n denotes the Chern number of band $|\varepsilon_-\rangle$. This suggests that σ_n behaves like the conventional Hall conductance. In fact,

as will be seen below, the response of the two-band system to the photon number in the field witnesses the transition points of the system.

In addition, we may define a response of the topological insulator to the mean amplitude of the field, taking the quantum part of the field into account. Namely, define

$$\sigma_q = \frac{\partial j(\bar{E}, \delta_E, n)}{\partial \bar{E}} \Big|_{E=0} \quad (11)$$

to characterize the response of the two-band system to the

classical part of the field. Simple algebra shows that, $\sigma_q = \frac{e^2}{\hbar} \int \frac{dk_x dk_y}{(2\pi)^2} \cos \alpha_q^- \Omega_{xy}^-(\vec{k})$. A limiting case for σ_q is that $\sigma_c = \sigma_q|_{\delta_E=0} = \left. \frac{\partial j(\vec{E}, \delta_E, n)}{\partial \vec{E}} \right|_{\vec{E}=\delta_E=0}$ quantifies the linear response of the insulator to the mean amplitude \vec{E} without quantum fields. Clearly, with $\delta_E = 0$ and $\omega \rightarrow 0$, we have $\eta = 0$ and $\cos \alpha_q^- = 1$. In this case, $\sin \alpha_c \approx \frac{gc}{|d|}$, and σ_c reduces to the well-known result,

$$\sigma_c = \frac{e^2}{\hbar} \int \frac{dk_x dk_y}{(2\pi)^2} \Omega_{xy}^-(\vec{k}).$$

We should notice that σ_c is exactly the conventional Hall conductance, while σ_q can be understood as the Hall conductance under the influence of quantum fluctuations. In this sense, we interpret σ_q as the Hall conductance in quantized fields, and σ_n quantifies the response of the two-band system to photon number of the field. In the next section, we will exemplify these responses with concrete examples.

III. EXAMPLES

For an explicit discussion on the Hall conductance, we first consider the following choices of $\vec{d}(\vec{k})$, $d_x = \sin k_y$, $d_y = \sin k_x$, $d_z = 2 - \cos k_x - \cos k_y - e_s$ [21]. Physically, this

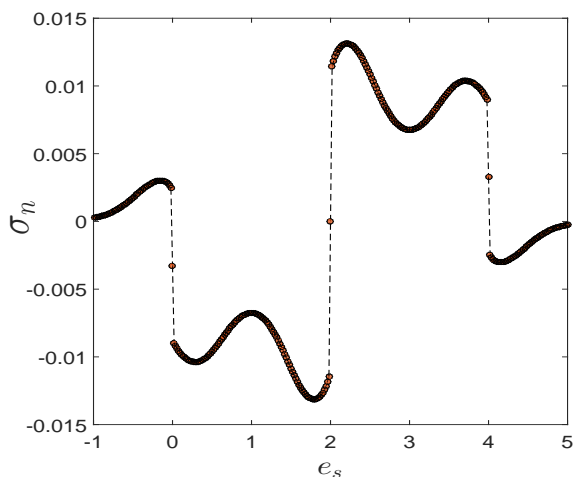


FIG. 1: (Color online) σ_n (in units of $\frac{e^2}{h}$), which quantifies the response of the system to the quantized part of field, as a function of e_s in a model with $d_x = \sin k_y$, $d_y = \sin k_x$, $d_z = 2 - \cos k_x - \cos k_y - e_s$. The other parameters chosen are $\delta_E = 0.3$ meV/nm, $\vec{E} = 0.1$ meV/nm.

model can be interpreted as a tight-binding model describing a magnetic semiconductor with Rashba type spin-orbit coupling, spin dependent effective mass and a uniform magnetization on z -direction. It has been shown[21] that $\sigma_c = 1$ for $0 < e_s < 2$; $\sigma_c = -1$ for $2 < e_s < 4$, and $\sigma_c = 0$ for $e_s < 0$ and $e_s > 4$.

With respect to the photon number n , the Hall conductance σ_n defined in Eq. (9) is plotted as a function of e_s in Fig.

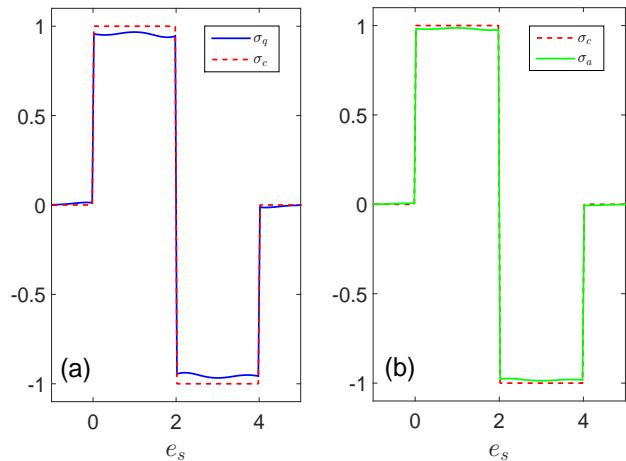


FIG. 2: (color online) (a) Hall conductance σ_q (in units of e^2/h) as a function of e_s , $\delta_E = 0.3$ meV/nm, $n = 4$. For comparison, the conventional Hall conductance (red-dashed line) is also shown. (b) Averaged Hall conductance σ_a as a function of e_s . σ_a is defined as $\sigma_a = \frac{1}{N} \sum_{j=1}^N \sigma_q(\delta_E^j)$, where δ_E^j denotes the j -th random value of δ_E from $[-0.3, 0.3]$. Here $N = 50$. $\vec{d}(\vec{k})$ is the same as in Fig. 1.

1. We find that the phase transition points, i.e., $e_s = 0, 2, 4$ remain unchanged. In contrast with the well known Hall conductance σ_c shown in Fig. 2 (red dashed lines), σ_n is not a constant in regions, $0 < e_s < 2$, $2 < e_s < 4$, $e_s < 0$ and $e_s > 4$. This results from the weight $\frac{\partial \cos \alpha_q^-}{\partial n}$ in the integral of Eq. (10). Physically, the weight plays the role of distribution function, which is not a constant and depends on k_x , k_y and e_s in this model. Fig. 2 shows σ_c , σ_a and σ_q as a function of e_s , where σ_a is defined as $\sigma_a = \frac{1}{N} \sum_{j=1}^N \sigma_q(\delta_E^j)$. δ_E^j denotes the j -th value of δ_E randomly chosen from $[-0.3, 0.3]$, that is, σ_a is defined as an average over δ_E chosen randomly in interval $[-0.3, 0.3]$. Two observations can be made. (1) Quantum fluctuations suppress the Hall conductance σ_c , but they do not change the phase transition points; (2) σ_a is very close to σ_c , suggesting that the quantum fields (fluctuations of the classical field) have small effect on the Hall conductance on average.

The second example we will take to illustrate the conductances is a two-dimensional lattice in a magnetic field [22]. The tight-binding Hamiltonian for such a lattice takes, $H = -t_a \sum_{\langle i,j \rangle} x c_j^\dagger c_i e^{i\theta_{ij}} - t_b \sum_{\langle i,j \rangle} y c_j^\dagger c_i e^{i\theta_{ij}}$, where c_j is the usual fermion operator on the lattice. The phase $\theta_{ij} = -\theta_{ji}$ represents the magnetic flux through the lattice. When $t_b = 0$, the single band is doubly degenerate. The term with t_b in the Hamiltonian gives the coupling between the two branches of the dispersion. Consider two branches which are coupled by $|l|$ -th order perturbation, the gaps open and the size of the gap due to this coupling is the order of $t_b^{|l|}$. The effective Hamiltonian then take the form of Eq. (1) with $d_x = \delta \cos k_y$, $d_y = \delta \sin k_y$, $d_z = 2t_a \cos(k_x + 2\pi mp/q)$, where p, q are integers, δ is proportional to (is the order of) $t_b^{|l|}$.

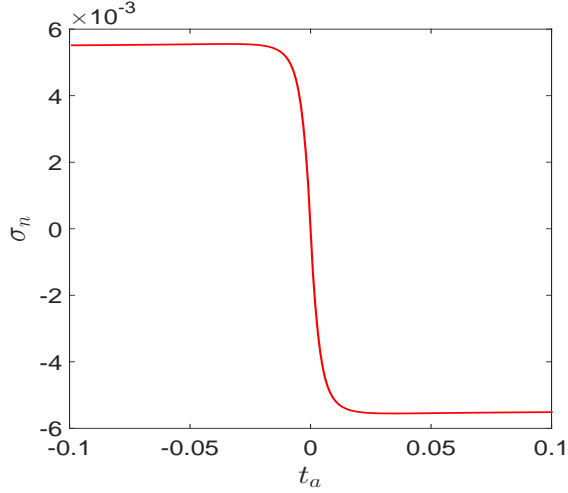


FIG. 3: (Color online) σ_n (in units of $\frac{e^2}{h}$) as a function of t_a . In this model, $d_x = \delta \cos k_y, d_y = \delta \sin k_y, d_z = 2t_a \cos(k_x + 2\pi mp/q)$. The other parameters are $\delta_E = 0.3$ meV/nm, $\bar{E}=0.1$ meV/nm, $m = 1, p = 1, q = 4, \delta = 0.01$ meV.

From Fig. 3, we observe that σ_n is very small, but it can witness the phase transition points. Fig. 4 shows the conventional Hall conductance σ_c , the Hall conductance σ_q subject to the quantized field, and the averaged Hall conductance σ_a as a function of t_a . We find that the transition points remain unchanged, but the Hall conductance is slightly changed. The features observed from Fig. 3 and Fig. 4 support the conclusions made in Fig. 1 and Fig. 2. These observations suggests that the quantum Hall effect can be taken as a method to determine the fine structure constant even in the presence of quantum fluctuations.

It is worth noticing that all hall conductance including σ_q , σ_c and σ_a are zero when $\bar{E} = 0$, since in this case,

$$\bar{v}_y = \sin^2 \frac{\alpha_{q0}}{2} \langle \varepsilon_+ | v_y | \varepsilon_+ \rangle + \cos^2 \frac{\alpha_{q0}}{2} \langle \varepsilon_- | v_y | \varepsilon_- \rangle = 0.$$

Here $\alpha_{q0} = \alpha_q^-(\bar{E} = 0)$. In other words, a quantized field can not induce current in the system. This feature is reminiscent of the which-way experiment[19, 20] that an attempt to gain information about the path taken by the particle inevitably reduces the visibility of the interference pattern. Here the quantum field can record the information of the path, while the classical field can not. Indeed, observing Eq.(7), we find that the current induced by the external field is very similar to the interference patten in the which-way experiment, where $|\varepsilon_+\rangle$ and $|\varepsilon_-\rangle$ play the role of the two paths.

Consider the case without photon in the field and neglect the vacuum effect, i.e., $n = 0$ and $\omega = 0$, the change in Hall conductances (with respect to the conventional Hall conductance) can be understood as a consequence of band mixing caused by the quantum field, since the bulk band gaps remain open, see Fig. 5. In Fig. 5, we plot the energy spectrum of the system in the first example. E_d denotes the spectrum of the system H_0 without external fields, E_c stands for the spectrum of the system in the external field with $\delta_E = 0$, and E_q is the

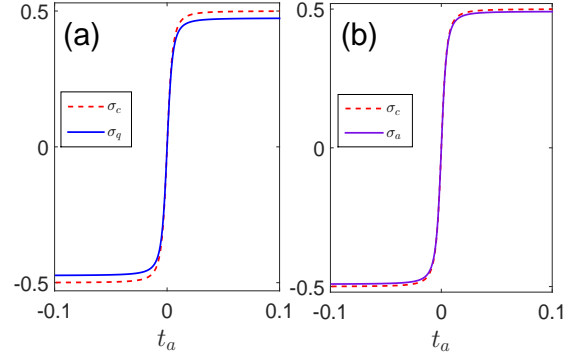


FIG. 4: (color online) (a) Hall conductance σ_q as a function of t_a . For comparison, the conventional Hall conductance σ_c is also plotted. The model is $d_x = \delta \cos k_y, d_y = \delta \sin k_y, d_z = 2t_a \cos(k_x + 2\pi mp/q)$. The other parameters chosen are $\delta_E = 0.3$ meV/nm. (b) Averaged Hall conductance σ_a versus t_a . σ_a is defined in the same way as in Fig. 2. δ_E is randomly chosen from $[-0.3, 0.3]$ meV/nm for 50 times. The other parameters chosen for both (a) and (b) are $m = 1, p = 1, q = 4, \delta = 0.01$ meV, $n = 4$. All conductances are plotted in units of $\frac{e^2}{h}$.

spectrum with $\delta_E \neq 0$. The interactions parameterized by \bar{E} and δ_E enlarge the band gaps. So, the topological nature of the system remains unchanged.

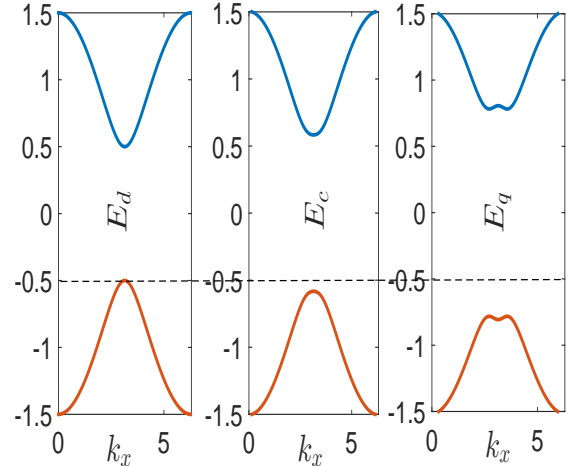


FIG. 5: (Color online) Energy spectrum (in units of meV) of the system in the first example. The other parameters are $e_s = 1.5$ meV, $\delta_E = \bar{E} = 0.3$ meV/nm, $n = 0, \omega = 0$.

The result changes when $n \neq 0$ and $\omega \neq 0$. The quantized field (or the photon field) can change the topology of the system, see Fig.6. It is possible to switch between different topological phases by changing the photon number and

the frequency, which may induces more avoid-crossing points as depicted in Fig.6. This observation is confirmed by an ac conductance $\sigma_q(\omega)$, which is defined in the same way as σ_q but without the limitation of $\omega \rightarrow 0$ in Eq. (8).

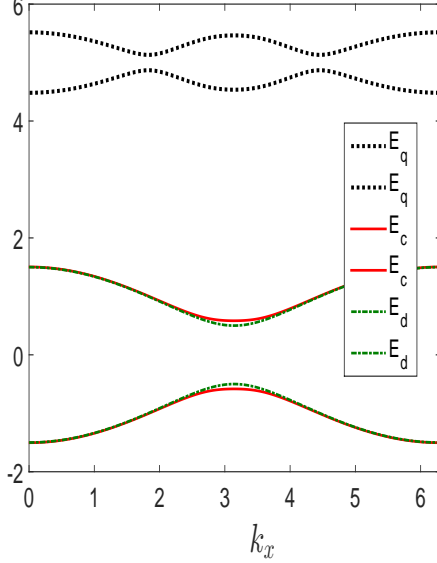


FIG. 6: (Color online) The same as Fig. 5, but with $\omega = 2, n = 1$.

To show the ac conductance of the system in the first example, we calculate $\sigma_q(\omega)$ as a function of e_s at various applied electric field frequencies ω . The numerical results are shown in Fig. 7. The difference between $\sigma_q(\omega)$ with various ω arises because the photon field may induce more avoid-crossing points, which is depicted in Fig.6, lines for E_q .

IV. DISCUSSION AND CONCLUSION

The two-band model may describe topological insulators, which is realized by using either condensed matter[23] or cold atoms settings[24]. The single mode field enters the system via a vector potential. The single photon mode is realized in a quantum LC circuit[25] or is selected from a ladder of cavity models by placing a dispersive element into the cavity, of which the reflective index is wave-vector dependent. Tuning frequency ω and the coupling of the field with ITs is possible by changing the dielectric constant. The Hall conductance (equivalently the Chern number) can be probed through a Thouless type[26]. The photon number may be tuned by a real-time quantum feedback procedure that generates on demand and stabilizes photon number states by reversing the effects of decoherence-induced quantum jumps[27]. Alternatively, the photon number may be tuned via changing the coupling constant, since the square root of the photon number $\sqrt{n+1}$ always appears with the coupling constant η .

In summary, we have introduced the response of a two-band system to a quantized single-mode field. Three types of Hall

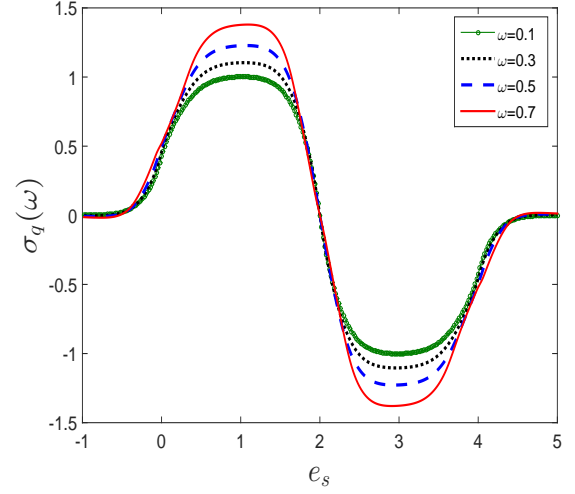


FIG. 7: (Color online) Hall conductance $\sigma_q(\omega)$ (in units of $\frac{e^2}{h}$) against e_s at various frequencies of the external field. In this plot, $d_x = \sin k_y, d_y = \sin k_x, d_z = 2 - \cos k_x - \cos k_y - e_s$. The other parameters are $\delta_E = 0.3$ meV/nm, $E_x = 0.1$ meV/nm, $n = 4$.

conductance are introduced to quantify this response. Two examples are presented to exemplify the theory. Physics behind the findings is revealed and discussed.

ACKNOWLEDGMENTS

This work is supported by National Natural Science Foundation of China (NSFC) under Grants No. 11175032, and No. 61475033.

Appendix A: The result beyond the RWA

In this APPENDIX, we will present discussions on the results beyond the Rotating-wave approximation (RWA). We start with the Hamiltonian in the maintext,

$$H = \sum_{j=\pm} E_j^c |E_j^c\rangle \langle E_j^c| + \hbar\omega a^\dagger a + \eta(a^\dagger + a)|E_+^c\rangle \langle E_-^c| + h.c. \quad (\text{A1})$$

Notations are the same as in the maintext. To solve this Hamiltonian, we transform H into an effective Hamiltonian,

$$H_{eff} = e^s H e^{-s} = \sum_{j=\pm} E_j^c |E_j^c\rangle \langle E_j^c| + \hbar\omega a^\dagger a + g' a |E_+^c\rangle \langle E_-^c| + h.c. \quad (\text{A2})$$

Here, $s = \frac{\Re(\eta)}{2E_+^c + \hbar\omega} \tau_x (a^\dagger - a) - \frac{\Im(\eta)}{2E_+^c + \hbar\omega} \tau_y (a^\dagger - a)$, and

$$g' = \frac{4E_+^c}{2E_+^c + \hbar\omega} \eta, \quad (\text{A3})$$

The eigenstates of the effective Hamiltonian are then,

$$|E_+^c\rangle'_n = \cos \frac{\alpha'_q}{2} e^{i\beta'_q} |E_+^c\rangle \otimes |n\rangle + \sin \frac{\alpha'_q}{2} |E_-^c\rangle \otimes |n+1\rangle,$$

and

$$|E_{-}^q\rangle'_n = \sin \frac{\alpha'_q}{2} e^{i\beta'_q} |E_{+}^c\rangle \otimes |n\rangle - \cos \frac{\alpha'_q}{2} |E_{-}^c\rangle \otimes |n+1\rangle,$$

with α'_q being defined by,

$$\cos \alpha'_q = \frac{(2E_{+}^c - \hbar\omega)}{\sqrt{\Delta^2 + 4|g'|^2(n+1)}},$$

and $\Delta = (2E_{+}^c - \hbar\omega)$. The corresponding eigenenergies are denoted by $E_{+}^{q'}(n)$ and $E_{-}^{q'}(n)$, respectively. Assuming band

$|E_{-}^q\rangle'_n$ is filled, we may calculate the current and the Hall conductance discussed above. Obviously, the Hall conductance takes the same formula except α'_q . The difference between α'_q and α_q originates from the coupling constant $g' = \frac{4E_{+}^c}{2E_{+}^c + \hbar\omega} \eta$. For points $\{\vec{k}\}$ satisfying (resonant condition) $2E_{+}^c = \hbar\omega$, we have $g' = \eta$, i.e., no difference g' and η at these resonant points. However, for the off-resonant points, g' and η might be very different, which can lead to different topological phases.

-
- [1] K. v. Klitzing, G. Dorda and M. Pepper, Phys. Rev. Lett. **45**, 494 (1980).
- [2] D. C. Tsui, H. L. Störmer and A. C. Gossard, Phys. Rev. Lett. **48**, 1559 (1982).
- [3] C. Nayak, S. H. Simon, A. Stern, M. Freedman and S. Das Sarma, Rev. Mod. Phys. **80**, 1083(2008); A. Y. Kitaev, Ann. Phys. **303**, 2(2003); A. Stern and N. H. Lindner, Science **339**, 1179(2013).
- [4] M. Z. Hasan and C. L. Kane, Rev. Mod. Phys. **82**, 3045 (2010), and references therein.
- [5] X. L. Qi, and S. C. Zhang, Phys. Today, **63**, 33(2010).
- [6] D. J. Thouless, M. Kohmoto, M.P. Nightingale, and M. den Nijs, Phys. Rev. Lett. **49**, 405(1982).
- [7] F. D. M. Haldane, Phys. Rev. Lett. **61**, 2015(1988).
- [8] B. A. Bernevig, T. L. Hughes, and S. C. Zhang, Science **314**, 1757(2006).
- [9] M. König, S. Wiedmann, C. Brüne, A. Roth, H. Buhmann, L. Molenkamp, X. L. Qi, and S.-C. Zhang, Science **318**, 766 (2007).
- [10] A. Roth, C. Brüne, H. Buhmann, L. W. Molenkamp, J. Maciejko, X. L. Qi, and S. C. Zhang, Science **325**, 294(2009).
- [11] X. L. Qi and S. C. Zhang, Rev. Mod. Phys. **83**, 1057 (2011).
- [12] R. Kubo, J. Phys. Soc. Jpn. **12**, 570 (1957).
- [13] D. J. Thouless, Phys. Rev. B **27**, 6083(1983).
- [14] M. V. Berry and J. M. Robbins, Proc. R. Soc. Lond. A **442**,659(1993).
- [15] O. V. Kibis, Phys. Rev. B **81**, 165433 (2010); O. V. Kibis, Phys. Rev. B **86**, 155108 (2012).
- [16] B. Dora, J. Cayssol, F. Simon, and R. Moessner, Phys. Rev. Lett. **108**, 056602 (2012).
- [17] M. Trif and Y. Tserkovnyak, Phys. Rev. Lett. **109**, 257002 (2012).
- [18] B. Gulasci and B. Dora, Phys. Rev. Lett. **115**, 160401 (2015).
- [19] S. Durt, T. Nonn, and G. Ramp, Nature **395**, 33(1998).
- [20] E. Buks, R. Schuster, M. Heiblum, D. Mahalu, V. Umansky, Nature **391**, 871(1998).
- [21] X. L. Qi, Y. S. Wu, and S. C. Zhang, Phys. Rev. B **74**, 085308(2006).
- [22] M. Kohmoto, Phys. Rev. B **39**, 11943 (1989).
- [23] N. H. Lindner, G. Refael, and V. Galitski, Nat. Phys. **7**, 490 (2011).
- [24] L. Jiang, T. Kitagawa, J. Alicea, A. R. Akhmerov, D. Pekker, G. Refael, J. I. Cirac, E. Demler, M. D. Lukin, and P. Zoller, Phys. Rev. Lett. **106**, 220402 (2011); N. Goldman, I. Satija, P. Nikolic, A. Bermudez, M. A. Martin-Delgado, M. Lewenstein, and I. B. Spielman, Phys. Rev. Lett. **105**, 255302 (2010); F. Wilczek, Phys. Rev. Lett. **109**, 160401 (2012).
- [25] K. Hepp and E. H. Lieb, Phys. Rev. A **8**, 2517 (1973).
- [26] J. Ye and C. Zhang, Phys. Rev. A **84**, 023840 (2011).
- [27] C. Sayrin, I. Dotsenko, X. Zhou, B. Peaudecerf, T. Rybarczyk, S. Gleyzes, P. Rouchon, M. Mirrahimi, H. Amini, M. Brune, J. Raimond, S. Haroche, Nature **477**, 73(2011).